

A mouse model for Down syndrome exhibits learning and behaviour deficits

Roger H. Reeves¹, Nicholas G. Irving¹, Timothy H. Moran², Anny Wohn², Cheryl Kitt³, Sangram S. Sisodia³, Cecilia Schmidt⁴, Roderick T. Bronson⁴ & Muriel T. Davisson⁴

Trisomy 21 or Down syndrome (DS) is the most frequent genetic cause of mental retardation, affecting one in 800 live born human beings. Mice with segmental trisomy 16 (Ts65Dn mice) are at dosage imbalance for genes corresponding to those on human chromosome 21q21-22.3—which includes the so-called DS 'critical region'. They do not show early-onset of Alzheimer disease pathology; however, Ts65Dn mice do demonstrate impaired performance in a complex learning task requiring the integration of visual and spatial information. The reproducibility of this phenotype among Ts65Dn mice indicates that dosage imbalance for a gene or genes in this region contributes to this impairment. The corresponding dosage imbalance for the human homologues of these genes may contribute to cognitive deficits in DS.

Departments of
¹Physiology,
²Psychiatry and
³Pathology, The
Johns Hopkins
University School of
Medicine, 725 N.
Wolfe Street,
Baltimore,
Maryland 21205,
USA and
⁴The Jackson
Laboratory, Box
258, Bar Harbor,
Maine 04609, USA

N.G.I. present
address:
Department of
Neurology, Institute
of Psychiatry,
London SE5 8AF,
UK

Correspondence
should be addressed
to R.H.R. or M.T.D.

Trisomy 21 is the most frequently observed aneuploidy among live born infants¹. DS produces a variety of developmental anomalies² including facial dysmorphology, congenital defects of heart and gut, infertility, immunodeficiencies and an increased incidence of leukaemia. Brain development is markedly affected. Grossly, brain weight is reduced, disproportionately so for cerebellum and brain stem³. Neuronal number is reduced in many regions and abnormal neuronal morphology is noted, especially in cerebral cortex. The brains of DS individuals exhibit neuropathology indistinguishable from Alzheimer disease by the end of the fourth decade⁴⁻⁸. DS is a leading genetic cause of mental retardation and places a substantial burden on affected individuals, their families and society.

A major goal of DS research is to correlate dosage imbalance of specific genes from human chromosome 21 with different clinical aspects of the syndrome. Substantial progress toward regional localization of such genes has come through the analysis of individuals with segmental trisomy 21 arising from translocations or duplications resulting in triplication of a subset of the chromosome⁹⁻¹¹. However, the resolution of this approach is limited by the substantial phenotypic variability among DS individuals and the very small number of well-characterized cases of 'translocation DS'⁹. A thorough analysis of the developmental consequences of DS requires an animal model that can provide access to cells and tissues from all developmental stages.

Comparative mapping between mice and humans has revealed that human chromosome 21 shares a large region of genetic homology with mouse chromosome 16 (Chr 16) (ref. 12). This observation led to the use of mice

trisomic for Chr 16 as an animal model of DS¹³. The trisomy 16 (Ts16) mouse exhibits some characteristics of DS, however, its value as a model is limited by several factors. First, Ts16 mice die *in utero*, precluding many types of analyses, especially of the development and function of the central nervous system. Second, murine homologues of the distal 2-3 Mb of human chromosome 21 are found on mouse chromosomes 17 and 10. In addition, Chr 16 contains a number of genes found on human chromosomes other than 21. Thus, Ts16 mice are not trisomic for some human chromosome 21 genes and are at dosage imbalance for many genes that are not implicated in the pathogenesis of DS.

A new mouse model of DS has been proposed. We generated a reciprocal translocation, T(16C3-4;17A2)65Dn (hereafter T65Dn), which can be used to produce segmental trisomy for distal Chr 16 (ref. 14). Cytological examination shows that the large 16¹⁷ T65Dn translocation product includes most of Chr 16 and nearly all of Chr 17, while the reciprocal 17¹⁶ product is a small marker chromosome containing the distal segment of Chr 16 translocated very close to the centromere of Chr 17. Missegregation of the 17¹⁶ chromosome in female translocation heterozygotes produces mice with segmental trisomy, Ts(17¹⁶)65Dn (Ts65Dn mice). These mice display a variety of phenotypic abnormalities, including early developmental delay evidenced by reduced birth weight, muscular trembling, male sterility and abnormal facies¹⁵.

To evaluate Ts65Dn mice as a model for studies of DS, somatic cell hybrids were constructed and used to map the Chr 16 breakpoint of the T65Dn translocation. The 17¹⁶ translocation chromosome contains genes from Chr 16 representing most of the segment evolutionarily

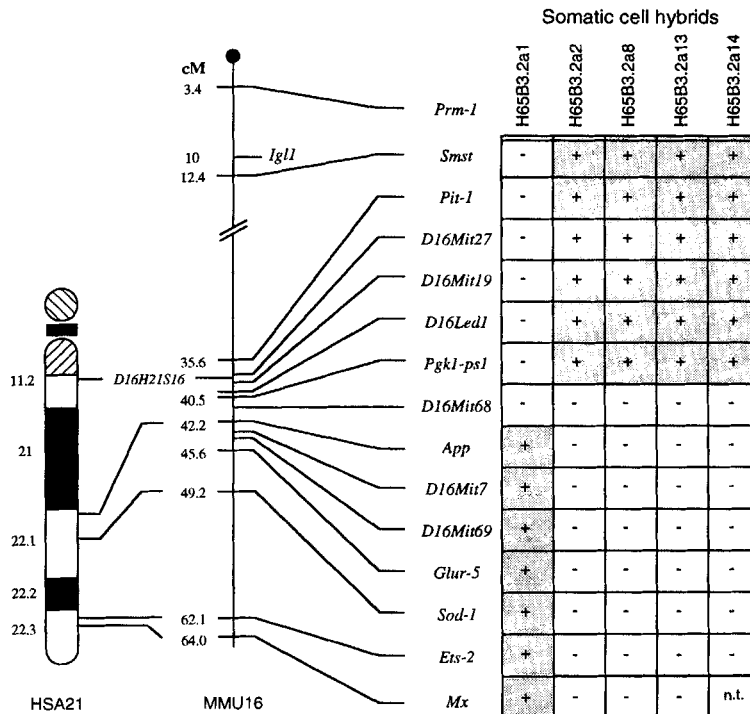


Fig. 1 The T(16;17)65Dn translocation breaks Chr 16 between *Pgk1-ps1* and *App*. Markers present (+) or absent (-) from five somatic cell hybrid lines segregating the reciprocal products of the T65Dn translocation are shown. A sex-averaged recombinational map of Chr 16 including distance from the centromere of several loci is included for reference (unpublished observations)¹². The positions of *Prm1*, *Igl1* and *D16H21S16* are included for reference. Relative positions of several markers on the cytological map of human chromosome 21 (HSA21) are indicated.

conserved with the long arm of human chromosome 21, while markers close to the centromere of Chr17 are absent. Two representative genes from the segment are expressed at elevated levels in Ts65Dn animals, demonstrating that sequences on the marker chromosome are transcriptionally active. Ts65Dn mice do not display some DS-associated phenotypes such as cardiac and skeletal anomalies, and no leukaemic Ts65Dn mice have been reported. We did not find pathology like that of Alzheimer's disease in animals up to 21 months of age. However, evaluation of the performance of Ts65Dn mice in a variety of behavioural tests demonstrates that segmental trisomy 16 results in spontaneous locomotor hyperactivity and impaired performance on a complex visual spatial learning and memory task. Thus, the Ts65Dn mouse has a genetic basis analogous to that of humans with segmental trisomy 21 and demonstrates behavioral abnormalities consistent with DS. This model will be valuable for studies of a variety of developmental problems that occur in DS.

Identification of the T65Dn breakpoint

Primary PRGS⁺ (phosphoribosyl glycinamide synthase⁺) fibroblasts from a mouse with one copy each of normal Chr16 and 17 and the reciprocal 16¹⁷ and 17¹⁶ products of the T65Dn translocation were fused to neomycin-resistant, PRGS⁻ (purine-dependent) AdeC-neo hamster cells. Somatic hybrids were selected in purine-free medium supplemented with G418. Three primary hybrids containing both the proximal Chr 16 gene, *Smst*, and a distal gene, *Ets2*, were passed through two rounds of subcloning by limiting dilution in non-selective medium. Thirty-nine subclones were recovered and typed for the proximal and distal markers. Four hybrid lines, H65B3.2a-2, -8, -13, and -14, were positive for *Smst* and negative for *Ets2*, demonstrating that they had lost both normal Chr 16 and the small 17¹⁶ translocation product but retained the large 16¹⁷ chromosome. One line, H65B3.2a-1, showed

the reciprocal pattern and thus retained the marker chromosome (17¹⁶) responsible for segmental trisomy in Ts65Dn mice as the only Chr 16 information in the cell.

The genetic position of the breakpoint was localized by typing the hybrids with 12 additional markers spanning the chromosome (Fig. 1). All four of the 16¹⁷ hybrids were positive for *Pgk-ps1* and five markers proximal to it, while the 17¹⁶ hybrid was negative for these markers and positive for *App*, *D16Mit7* and *D16Mit69*, *Grik1*, *Sod1*, *Ets2* and *Mx1*, the most distal marker mapped on Chr 16. Surprisingly, the marker *D16Mit68*, which maps between *App* and *Pgk-ps1* on the recombinational map of Chr 16 (ref. 12), was absent from all five hybrids. *D16Mit68* was a robust marker that generated the expected 210 bp fragment from DBA/2J mice (the strain in which T65Dn was induced) and from an independent set of mouse X-hamster somatic cell hybrids segregating a different Chr 16 translocation (not shown). The absence of this marker from the T65Dn hybrids suggests that a small portion of Chr 16 surrounding the translocation breakpoint may have been deleted from the chromosome at the time of the translocation. This would place the actual breakpoint at the *D16Mit68* locus, which is 0.7 cM proximal to *App* on a composite map of Chr 16 (ref. 12).

Two markers of proximal Chr 17 were mapped in the hybrids (data not shown). *D17Mit58* is located 1.1 cM from the centromere of Chr 17 on the M.I.T. reference panel and *D17Mit34* maps 10.0 cM from the centromere¹⁶. Both markers were absent from hybrids containing the small marker chromosome and present in hybrids containing the larger 16¹⁷ translocation product. Thus, very little information from Chr 17 is at dosage imbalance in Ts65Dn mice.

Elevated expression of Chr 16 genes

KCN-sensitive superoxide dismutase (SOD) activity was measured in the livers of three Ts65Dn mice and four

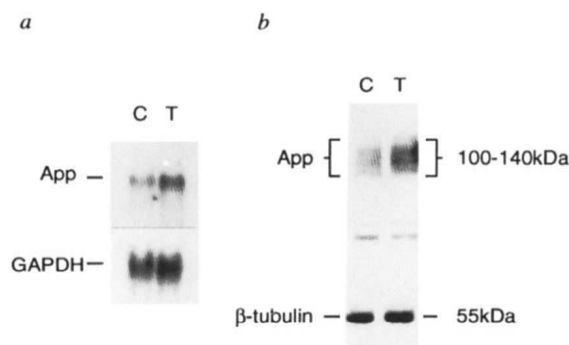


Fig. 2 *App* expression is elevated at the RNA and protein level in Ts65Dn mice. *a*, Northern blots of brain RNA were probed for *App* message, stripped, and reprobated with *Gapd*. Scanning densitometry was used to compare relative levels in control (C) and segmentally trisomic (T) animals. *b*, Western blots on total brain protein were analyzed with antibodies against the C-terminal end of APP and against β -tubulin. The CT15 antibody recognizes several APP variants that arise due to differential splicing of the message but share the same carboxy terminus.

euploid littermates. The mean activity was 2.31 ± 0.18 U/mg protein in segmentally trisomic mice compared with 1.68 ± 0.10 in normal controls. This 1.4-fold increase was significant ($P < 0.05$, $t = 3.359$ in a two-tailed t test). Thus, the increased copy number of *Sod1* genes in this segmental trisomy is reflected in the elevation of enzyme activity, as expected if genes on the 17¹⁶ marker chromosome are expressed.

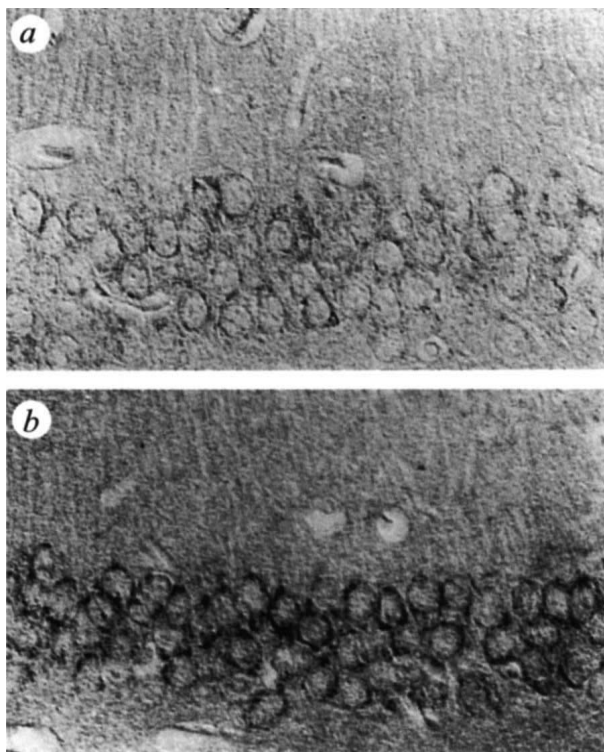


Fig. 3 APP expression in neurons is elevated but amyloid plaques are absent from the brains of Ts65Dn mice up to 21 months of age. Sagittal section of hippocampus from control (a) and Ts65Dn mouse (b) showing neurons after immunocytochemistry with the CT15 antibody directed against the C terminus of APP.

Quantitative northern blotting of RNA from cerebral cortex was used to compare the levels of *App* transcript in four euploid and three Ts65Dn mice (Fig. 2a). Filters were hybridized with the murine *App* cDNA clone, stripped, and reprobated with a control probe recognizing *Gapd*. The ratios of hybridization intensity were determined by scanning densitometry and the averages for Ts65Dn mice were compared to controls. This analysis demonstrated a 2.2-fold increase in *App* mRNA in the cortex of segmentally aneuploid adult animals, consistent with the 2.5-fold increase seen in cortex of trisomy 16 mice at fifteen days of gestation¹⁷. Concomitant elevation of APP protein was demonstrated in the same animals by western blotting using a polyclonal antibody, CT15, directed against the carboxy-terminal end of the molecule. Intensity of reactivity with a monoclonal antibody specific for β -tubulin served as a control (Fig. 2b). A significant, twofold increase in APP protein was observed.

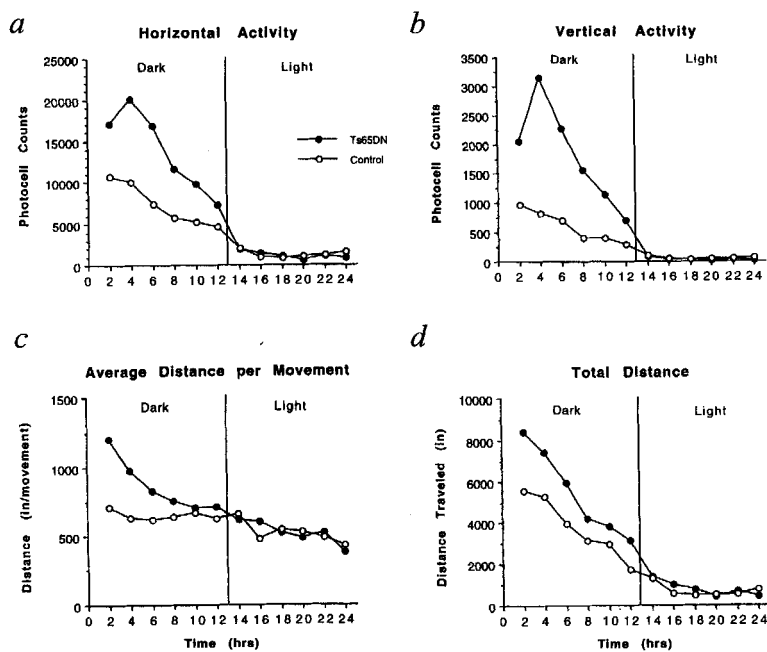
Allele of AD-like histopathology

Four control and six Ts65Dn animals ranging in age from 3 to 21 months were examined. Normal neuronal and glial integrity were observed on staining with three standard stains and there was no indication of neuritic plaques or neurofibrillary tangles on examination with Congo Red, Thioflavin T or Bielschowski silver staining. Immunohistochemistry also failed to reveal pathology reminiscent of that seen in Alzheimer disease. As expected from northern and western blotting studies, analysis with the CT15 antibody showed increased APP reactivity in Ts65Dn animals, especially in the hippocampus (Fig. 3). However, antibody 8E5, directed against the Ab peptide, and a second antibody against ubiquitin did not detect any abnormal deposits characteristic of senile plaques. No increase in GFAP was observed in the brains of Ts65Dn mice by immunocytochemistry or by northern blotting (data not shown). Screens with antibodies to synap-tophysin and to phosphorylated and non-phosphorylated epitopes of neurofilaments did not detect differences between control and trisomic animals and tyrosine hydroxylase reactivity appeared normal.

Spontaneous locomotor hyperactivity

Spontaneous activity of Ts65Dn and control mice of both sexes was similar on most variables during the habituation period, but was increased significantly in both the total distance and the average distance per movement variables in segmental trisomic animals (data not shown). Analysis of 24-hour activity also demonstrated significant hyperactivity in Ts65Dn mice compared with controls (Fig. 4). During the dark cycle, Ts65Dn mice of both sexes demonstrated significantly higher interruption of photocells in both the horizontal and vertical planes. The increase in horizontal activity translated into significantly greater locomotor activity as evidenced by higher levels of distance traveled and increased distance per movement. These increases were most evident in the first half of the dark cycle. There were no differences in activity during the light cycle as both Ts65Dn and control mice demonstrated normal diurnal activity patterns. The spontaneous hyperactivity demonstrated in the Ts65Dn mice is consistent with previous reports of hyperactivity in Ts16^{->2n} chimeras¹⁸. Spontaneous hyperactivity has been noted in a variety of rodent models of developmental and

Fig. 4 Patterns of spontaneous activity for 24 hours in combined male and female Ts65Dn and control mice (12 each, control and Ts65Dn). *a*, Horizontal activity: ANOVA demonstrated significant effects for sex [$F(1,18) = 10.308, P < .005$], genotype [$F(1,18) = 6.442, P < .02$], and time [$F(11,198) = 43.864, P < .001$] and significant sex \times time [$F(11,198) = 8.730, P < .001$] and genotype \times time [$F(11,181) = 5.674, P < .001$] interactions. Ts65Dn mice were significantly hyperactive relative to controls during the first 10 h of the dark cycle. Females of both Ts65Dn and control lines were hyperactive relative to males. *b*, Vertical activity: ANOVA demonstrated significant effects for sex [$F(1,18) = 6.297, P < .02$], and time [$F(11,198) = 12.212, P < .001$] and significant sex \times time [$F(11,198) = 4.927, P < .001$] and genotype \times time [$F(11,181) = 3.730, P < .001$] interactions. Ts65Dn mice were significantly hyperactive relative to controls during the first 8 h of the dark cycle. Females were relatively hyperactive compared with males in both Ts65Dn and control mice. *c*, Average distance per movement: ANOVA demonstrated significant effects for sex [$F(1,18) = 5.210, P < .05$] and time [$F(11,198) = 15.954, P < .001$] and a significant genotype \times time [$F(11,181) = 5.021, P < .001$] interactions. By this measure, Ts65Dn mice were hyperactive relative to controls during the first 6 hours of the dark cycle. Females were more active than males. There were no differences on any of the other behavioral variables. *d*, Total distance: ANOVA demonstrated significant effects for sex [$F(1,18) = 4.576, P < .05$], genotype [$F(1,18) = 6.553, P < .02$] and time [$F(11,198) = 97.353, P < .001$] and significant sex \times genotype [$F(1,18) = 4.985, P < .05$], sex \times time [$F(11,198) = 4.927, P < .001$] and genotype \times time [$F(11,181) = 3.730, P < .001$] interactions. Overall, Ts65Dn mice were significantly hyperactive relative to controls during the first 6 h of the dark cycle. This was due to significant hyperactivity in male Ts65Dn mice relative to controls.



neurodegenerative disorders^{19–21} and appears to be a nonspecific marker of disordered CNS development.

Impaired performance in the Morris water maze

In the first phase of the task, the location of the platform was indicated by a flag. Although Ts65Dn mice demonstrated significant decreases in search time over the 6 trials, their performance remained significantly impaired relative to controls throughout testing (Fig. 5*a*). When placed into the hidden platform version of the task (Fig. 5*b*), control mice demonstrated significant carryover from the visible platform component and quickly mastered the task. In contrast, Ts65Dn mice initially performed no better than before visible platform training and their performance remained significantly poorer than that of controls throughout the nine trials. Both controls and Ts65Dn mice demonstrated a knowledge of the platform position as indicated by higher searching times in the quadrant containing the platform than in other quadrants in the tank (Fig. 5*c*). Even in this aspect of the task, however, the performance of the Ts65Dn mice was significantly impaired relative to controls. Thus, while the Ts65Dn mice were able to acquire aspects of the Morris water maze task, their performance remained significantly impaired relative to controls.

Discussion

The Ts65Dn mouse represents a new animal model for Down syndrome. These mice possess extra genetic information from the region of distal Chr 16 corresponding to human chromosome 21q21–22.1. Comparative maps

of these regions 18 loci mapped in the same or consistent orders, including *App*, *Grik1*, *Sod1*, *D16H21S58*, *Gart*, *Son*, *Igft*, *Ifnar*, *Crf2-4*, *Gas4*, *Kcne1*, *Cbr*, *Pcp4*, *Erg*, *Ets2*, *Hmg14*, *Mx2* and *Mx1* (ref. 12). Cytological examination indicates that approximately 7–10% of Chr 16, or about 9–12 Mb, is present in the small translocation product and thus is present at dosage imbalance in Ts65Dn animals. Estimates of the physical distance from *APP* to *MX1* in the corresponding region of chromosome 21 in humans are on the order of 15 Mb on the *NotI* map²² and 12 Mb as measured on radiation hybrid lines²³.

Ts65Dn mice are not at dosage imbalance for the homologues of all genes on human chromosome 21, and thus are more analogous to human beings with translocation DS than with full trisomy 21. Three loci mapped to both human 21 and Chr 16, the anonymous DNA segments, *D16H21S13*, *D16H21S16*, and *D16H21S52* (ref. 24), are not included in the 17¹⁶ marker chromosome, and genes distal to *MX1* on HSA21 are found on mouse Chr 17 and 10. Dosage imbalance for Chr 17 genes carried on the T65Dn translocation may also contribute to the Ts65Dn phenotype. However, markers of the most proximal Chr 17 locus identified by the M.I.T. genome effort¹⁶ were absent from the 17¹⁶ marker chromosome, suggesting that this contribution is minimal.

Careful assessment of the clinical phenotypes of individuals with partial duplications of HSA21 have been used to correlate dosage imbalance of specific regions of human chromosome 21 with many aspects of the DS phenotype, including characteristic cardiac anomalies and mental retardation⁹. The heart defects characteristic

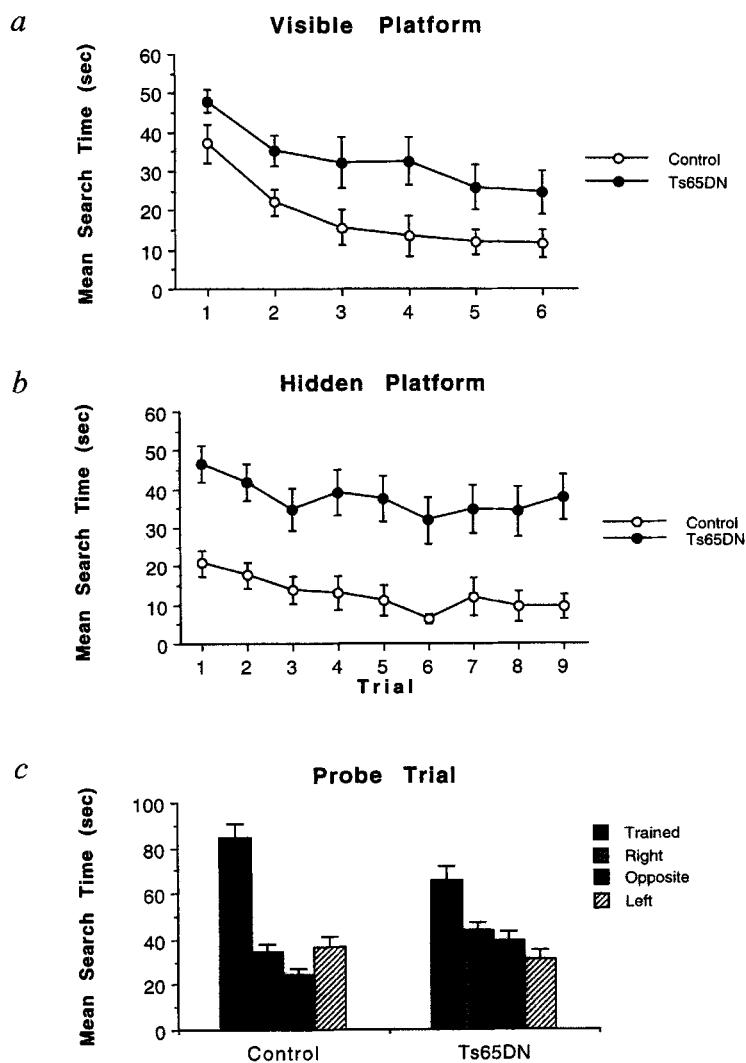


Fig 5. 12 Ts65Dn and 12 control mice were tested in the Morris water maze. *a*, Visible platform: Mean search time across trials for combined male and female Ts65Dn and control mice when the position of the platform is cued by the presence of a flag above the surface of the tank. ANOVA demonstrated significant effects of genotype [$F(1,19) = 7.109, P < .02$] and time [$F(5,95) = 21.887, P < .001$]. There was significant improvement over trials in both Ts65Dn mice [$F(5,95) = 8.508, P < .001$] and control mice [$F(5,95) = 15.121, P < .001$]. Ts65Dn mice took significantly longer to locate the visual platform on all but the first of the 6 trials. *b*, Hidden platform: Mean search time across trials in combined male and female Ts65Dn and control mice when the position of the platform is hidden. ANOVA demonstrated significant effects of genotype [$F(1,19) = 21.831, P < .001$] and time [$F(8,152) = 3.991, P < .001$]. Ts65Dn took significantly longer to locate the hidden platform at all trials. *c*, Morris water maze probe trial: Amount of time spent searching in four quadrants of the swim tank relative to the platform position during training. ANOVA indicated significant position preferences [$F(3,57) = 35.094, P < .001$] and a significant genotype x position interaction [$F(3,57) = 4.571, P < .01$]. Analyses of simple effects indicated that Ts65Dn mice spent significantly less time searching in the quadrant that had contained the platform than did control mice [$F(1,57) = 8.332, P < .005$].

of Ts16 (and DS) have not been observed in live born Ts65Dn mice, raising the question of whether these anomalies are analogous to those observed in 30–50% of liveborn individuals with DS. In both humans and mice, the specific defects in development of the atrial-ventricular septa are extremely rare except in DS or Ts16, although associated outflow tract problems are more common in both species. In contrast to the variable frequency of cardiac anomalies in DS, these defects were observed in nearly 100% of mouse embryos that were trisomic for all of Chr 16 on a C57BL/10 background²⁵. Ts65Dn mice are not inbred but are maintained by mating carriers of the 17¹⁶ chromosome to B6EiC3HF1 hybrid mice, producing trisomy on a variable genetic background. In Ts65Dn mice and in DS individuals, the variable genetic background may ameliorate cardiac defects in many individuals. Alternatively, the Ts16 cardiac defect may be due to genes outside the region of human 21 homology. A region of proximal Chr 16 is homologous to HSA22q11, deletion of which is correlated with cardiac defects in velo-cardio-facial and DiGeorge syndromes^{26,27}.

The occurrence by the age of 35 or 40 of neuritic plaques and tangles characteristic of AD is among the few attributes common to all individuals with DS²⁸. So far, there is no information from translocation DS individuals that would help to localize genes contributing to the development of

AD-like histopathology. The *APP* gene has been associated with AD because a cleavage product of this protein is the major constituent of neuritic plaques^{29,30}, because specific *APP* mutations are found in rare familial forms of early-onset AD^{31,32}, and circumstantially because *APP* levels are elevated in DS individuals⁵. Transgenic mice that express elevated levels of the complete human *APP* protein from the normal promoter do not develop AD-like pathology³³, but animals expressing a mutant form of *APP* at very high levels from a heterologous promoter are able to form neuritic plaques like those in AD³⁴. The absence of this neuropathology from Ts65Dn mice raises the possibility that the invariant early-onset AD phenotype of DS may stem in part from dosage imbalance of chromosome 21 genes not represented on the 17¹⁶ chromosome.

In contrast to the brains of individuals with DS, the Ts65Dn brain displayed minimal gross pathological alterations (manuscript in preparation). However, Ts65Dn mice displayed a significant performance deficit on the Morris water maze. While they were able to learn both the visible and hidden platform components of the task, they showed significant deficits relative to controls. Euploid mice demonstrated significant carry-over from the visible to the hidden platform components, while the initial search times of Ts65Dn mice in the hidden platform task were not improved at all by prior conditioning. Many

types of disruption to the hippocampus impair performance in the hidden platform but not the visible platform component of the task³⁵. Thus the deficits exhibited by the Ts65Dn mice appear not to be specific for hippocampus. The Morris water maze is commonly used for assessing spatial learning and memory that uses the relationship among stimuli to guide behaviour. It requires the development of an effective search strategy, the identification of relevant stimuli, the memory of effective behaviour on previous trials and the integration of this information into appropriate performance. The impaired performance of Ts65Dn mice could result from a deficit in one or more of these components.

The severity of mental retardation varies substantially among DS individuals and can be influenced by the degree of environmental enrichment³⁶. While this individual variability complicates the characterization of cognitive deficits that result directly from trisomy 21, affected individuals perform less well on some tasks than on others. When compared to younger children of a similar mental age, DS individuals demonstrate deficits in auditory and visual spatial processing³⁷ and in short-term memory³⁸. Deficits in either visual spatial processing and/or short term memory would impair performance in the Morris water maze. In contrast to DS individuals, Ts65Dn mice show a relatively low level of individual variation in a specific learning/performance deficit resulting from a well-defined dosage imbalance of less than 0.4% of the mouse genome. Since Ts65Dn mice are maintained on a hybrid background, genetic homogeneity is apparently not a major factor accounting for this low variability. The reproducibility of this impairment suggests that a subset of genes in this region may affect brain development in a specific manner to result in these deficits. It is reasonable to suggest that dosage imbalance for the human homologues of these genes in human beings may contribute to cognitive deficits in DS individuals. Creation of dosage imbalance with transgenic mice containing yeast artificial chromosomes from human 21 or Chr 16 should provide a viable approach to further localization and identification of these genes^{33, 39}.

Our analysis establishes the genetic basis for the use of Ts65Dn mice as a viable animal model for studies of DS. In contrast to mice trisomic for all of Chr 16, Ts65Dn mice survive gestation and usually live to adulthood, and thus provide access to all cells, tissues and higher order processes at all stages of development. The ability to test cognitive performance provides a sensitive indicator of brain development and function, as well as a system for examination of the underlying physiological basis for differences between trisomic and euploid animals. Ts65Dn mice also provide a model for studying the aging process in DS, a critical concern in the face of an increasing average age of DS individuals. There are obvious differences in the specific end points of development between mouse and human beings that will determine some of the limits of this animal model. However, the patterns of sequential gene expression in development of all mammals share a common basis, and thus Ts65Dn mice provide an important biological model for the study of one of the most frequent genetic anomalies seen in human beings.

Methods

Mice and chromosome translocations. The production of the reciprocal translocation, T65Dn, has been described¹⁴. Briefly, DBA/

2J male mice were irradiated, mated to C57BL/6J females and their progeny screened for chromosomal anomalies involving Chr 16. Translocation breakpoints were identified in G-banded chromosomes of cultured peripheral lymphocytes⁴⁰. All mice used in this study were bred in the Robertsonian Chromosome Resource at The Jackson Laboratory. Ts65Dn animals were generated by mating segmentally trisomic females to (C57BL/6EiJ) × C3H/HeJ F1 males each generation. Because C3H/HeJ mice carry a mutation resulting in retinal degeneration (*rd*), all mice used in behavioral studies were confirmed to have intact retinas by direct analysis of the *rd* gene⁴¹, examination of the retina by slit lamp, or both. Ts65Dn mice are available from the Jackson Laboratory.

T65Dn cell strains. Primary fibroblast cell strains were established from lung, liver, spleen and testis of young adult heterozygous mice carrying both products of the reciprocal translocation, T65Dn. The organs were minced in sterile phosphate buffered saline with repeated rinsing to remove red blood cells. Washed tissue pieces were transferred to gelatin coated tissue culture dishes, fed with Dulbecco's MEM supplemented with 10% fetal calf serum and antibiotics, and cultured in a 37 °C incubator in 10% CO₂ atmosphere. When robust cell growth was seen in a dish (generally 1–2 weeks after plating), the cells were trypsinized and split 1:2. In general, cells from one original dish were expanded through 3–4 passages in this manner.

Somatic-cell hybrids. AdeC-neo is a derivative of the hamster CHO cell line that is deficient in the purine salvage pathway enzyme, phosphoribosyl glycinamide synthetase (PRGS) encoded in the *Gart* complex on Chr 16 (ref. 42). Hybrids were made by polyethylene glycol-mediated fusion of AdeC-neo and T65Dn cells as described⁴². 24 h after fusion, the cells were trypsinized and split 1:10 into purine-free Ham's F12 medium (GIBCO) containing 400 µg ml⁻¹ of G418. Colonies appearing after 10–14 days were picked using cloning cylinders and expanded. Subcloning was accomplished by plating 10–100 cells per 100 mm² dish in non-selective Ham's F12 medium (with purines) and picking well-separated individual colonies with cloning cylinders.

Southern, northern and western blotting. DNA and RNA extraction, Southern and northern blotting, radiolabelled probe synthesis and hybridization were accomplished using standard procedures^{44, 45}. Probes included genomic clone pMST1.4 for preprosomatostatin, *Smt1*⁴⁵; the pks-Pit plasmid for the pituitary specific transcription factor, *Pit1*⁴⁶; a 700 bp *HindIII*–*PstI* fragment from clone CTH6p for *D16Led1* (ref. 47), kindly provided by Dr. Richard Chaillet; clone B24 containing the pseudogene, *Pgk1-ps1* (ref. 48); cDNA clone pDS10.1 containing 1 kb from the 3' end of an *App* cDNA clone¹⁷; a glutamate receptor (*Grik1*) mouse cDNA clone⁴³; cDNA for the cytoplasmic form of superoxide dismutase, *Sod1* (ref. 50); and a murine cDNA for the *Ets2* protooncogene, pA3-1.6 (ref. 51); genomic clone pMx 3.4 for *Mxl* (ref. 52). A cDNA clone for glyceraldehyde phosphate dehydrogenase, *Gapd*, was used in quantitative northern blotting experiments, which were carried out as described⁴⁴ except that a Molecular Dynamics scanning densitometer was used to quantify the intensity of hybridization with each probe. Three Ts65Dn and four control mice were used for each determination. PCR primers for the marker *D16Mit7* were reported by Dietrich *et al.*⁵³. Primers for *D16Mit19*, *D16Mit27*, *D16Mit68* and *D16Mit69* were obtained from Research Genetics. PCR reactions were performed using 500 nM or 1 µM primer⁵⁴. PCR products were separated on 3.5% low melting point agarose gels and visualized under UV light after staining with ethidium bromide.

For western blots, protein was extracted from the cortex of three Ts65Dn and four control mice in 8 M urea, 50 mM Tris-HCl, pH 7.2, 0.5% SDS, 1 mM PMSF. Proteins were separated on SDS-PAGE gels and transferred to nitrocellulose filters by electroblotting. Mouse *App* protein was detected using the polyclonal antibody, CT15, directed against the C-terminal 15 residues of *App*⁵⁵. Monoclonal antibody 18D8, which recognizes β-tubulin, was kindly provided by D. Cleveland and was used as an internal control for protein loading. Horseradish peroxidase-conjugated secondary antibodies were visualized by chemiluminescence using the ECL system (Amersham).

SOD1 assay. SOD1 activity was assayed using a spectrophotometric assay in which SOD1 inhibits the formation of nitrite from hydroxylammonium chloride⁵⁶. Reactions (500 µl) containing 250

μ l human SOD1 standard (Sigma) or cell extract in 65 mM phosphate buffer, 25 μ l xanthine (1.142 mg ml⁻¹), 75 μ l xanthine oxidase (0.1 U ml⁻¹), 25 μ l hydroxylammonium chloride (0.69 mg ml⁻¹), and 125 μ l KCN (4 mM) or H₂O were incubated at 25 °C for 20 min. 500 μ l anaphthylamine (1 ng ml⁻¹) and 500 μ l sulfanilic acid (3.3 mg ml⁻¹) were added and the mixtures were incubated for a further 20 min at 25 °C after which the OD was determined at 530 nm⁵⁷. KCN-sensitive SOD1 activity was calculated from the total activity minus the KCN-resistant activity. Total protein was determined by the method of Lowry, using standard protocols. One unit of enzyme activity is defined as the amount that inhibits the formation of nitrite by 50%.

Histology. Organs were fixed in 4% paraformaldehyde or Bouin's solution by perfusion or drop fixation and embedded in paraffin. Five to ten μ m thick sections were mounted onto Vectabond-treated glass slides, air dried overnight, deparaffinized and transferred through xylenes and alcohols to water. Selected sections were stained with hematoxylin and eosin, Congo red, cresyl violet, Luxol fast blue, thioflavin T or Bielschowski silver. For immunocytochemistry, slides were pretreated with H₂O₂ (3% in methanol) to block staining of endogenous peroxidases, and washed in deionized water. To enhance antigen detection, slides were irradiated in a conventional microwave at full power in H₂O for 15 min, cooled to r.t. and rinsed three times for 5 min each in 0.1 M PBS (pH 7.6). Sections were then incubated in 0.4% Triton X-100 (TX)/0.1% PBS for 5 min at r.t. and transferred to 10% normal horse or goat serum in 1% bovine albumin and 0.1% TX/0.1M PBS for 1 h at r.t. Primary antibody and control solutions were prepared in 0.1% TX/0.1 M PBS/10% normal horse or goat serum and incubated on the slide for 24 h at room temperature. Sections were rinsed in 0.1 M PBS followed by incubation in the appropriate avidin-conjugated horseradish peroxidase for 30 min at room temperature. Rinsed slides were reacted in the presence of 0.05% diaminobenzidine in 0.01% H₂O₂, rinsed in PBS, dehydrated through graded ethanols to xylenes and coverslipped. Primary antibodies included CT15 (ref. 54); 8E5, directed against the AD-specific Ab peptide (courtesy of D. Shank, Athena Neurosciences); SMI 31 and SMI 32 (Sternberger) against neurofilament protein; antibodies directed against synaptophysin (Biogenix), glial fibrillary acidic protein (GFAP) and tyrosine hydroxylase (Boehringer-Mannheim); and control sera including anti-mouse IgG (Cappel), anti-rabbit IgG (Vector), normal mouse serum (Sigma), and normal rabbit serum (Gibco).

Behavioural testing. Spontaneous activity over a 26 h period was examined in computerized Digiscan (Omnitech Electronics) activity monitors, clear Plexiglas cages measuring 16 × 16 × 12 inches with one row of infrared monitoring sensors mounted every 5 cm along the perimeter at the base and a second row of sensors mounted at a height of 10 cm. Data were collected and interpreted by a Digiscan computer connected to an Apple 2e computer for data storage and subsequent analysis. System differentiated behavioural variables recorded from each sampling interval included a) horizontal activity (total number of lower plane beam interruptions), b) total distance (in inches), c) movement time, d) rest time, e) speed of movement,

f) number of movements, g) mean distance per movement, h) vertical activity (total number of higher plane beam interruptions), i) vertical time, j) number of vertical movements, k) stereotype time, l) number of stereotypes, m) time spent in each of the 9 separate zones within the chamber. Animals were placed into the chambers 2 h prior to lights out and activity was monitored in 2 h intervals for 26 h. The first 2 h period was considered a habituation period and data from that interval were separately analyzed by 2-way ANOVA. Data from the subsequent 12 sampling intervals were analyzed by a mixed model ANOVA with genetic status and sex as independent variables and sampling interval as a repeated variable.

The Morris water maze consists of a circular swim tank 72 cm in diameter filled with water made opaque by the addition of non-toxic white latex paint. The tank is divided into 4 quadrants by the imposition of 4 patterns on the internal wall. A small platform (5 cm square) is placed in one of four quadrants, 1 cm below the surface of the water. The first test is a visible-platform task in which the position of the platform is signaled by the presence of a visually conspicuous 'flag' above the platform. The platform position varied among four possible positions within each block of trials and animals were tested on three blocks of trials per day for two days or a total of 24 trials. Blocks of trials were separated by 1 h. Animals were placed in the center of the tank and latency to locate the platform and escape from the water was the dependent measure. Animals not finding the platform within 60 s were placed on it for 30 s before the next trial.

Twelve days following completion of the visible-platform task, mice were tested on the hidden platform version of the task in which the platform was maintained in a fixed location and there was no flag identifying its position. Animals were placed into the tank around the perimeter in one of four start positions used in a semirandom fashion throughout the 4 trials per block. Mice were allowed to search the tank for 60 s and to remain on the platform for 30 s. If the platform was not located within 60 s, they were removed from the water and placed on the platform. Three blocks of trials were run on three consecutive days. As in the hidden platform task, escape latencies were the dependent variable.

In the final phase of testing, the platform was removed from the tank and trained mice were allowed to swim for 180 s. Time spent in each quadrant was ascertained to determine whether the majority of swimming occurred in the quadrant that previously contained the platform. Data from all components of the Morris water maze task were analyzed by mixed model ANOVA.

Acknowledgments

M. Citron provided excellent technical assistance. We thank J.D. Gearhart for thoughtful suggestions and support throughout the course of these studies and K. Johnson and W. Frankel for their careful reviews of the manuscript. This work was supported by Public Health Service awards HD24605 (RHR, THM, and MTD), HD13131 (MTD) and HG00405 (RHR).

Received 13 April; accepted 19 June 1995.

1. Hook, E.B. in *Trisomy 21 (Down Syndrome): Research Perspectives* (eds. Cruz, F.F.d.I. & Gerald, P.S.) 3–68 (University Park Press, Baltimore, 1981).
2. Coyle, J.T., Oster-Granite, M.L. & Gearhart, J.D. The neurobiological consequences of Down Syndrome. *Brain Res. Bull.* **16**, 773–787 (1986).
3. Crome, R., Cowie, V. & Slater, E. A statistical note on cerebellar and brainstem weight in Down Syndrome. *J. ment. Def. Res.* **10**, 69–72 (1966).
4. Solitaire, G. & Lamarche, J. Alzheimer's disease and senile dementia as seen in Mongoloids: neuropathological observations. *Am. J. ment. Def.* **70**, 840–848 (1966).
5. Haberland, C. Alzheimer's disease in Down syndrome. *Acta Neurol. Belgium* **69**, 369–380 (1969).
6. Ellis, W.G., McCulloch, J.R. & Corley, C.L. Presenile dementia in Down syndrome. Ultrastructural identity with Alzheimer's disease. *Neurology* **24**, 101–106 (1974).
7. Burger, P.C. & Vogel, F.S. The development of the pathologic changes of Alzheimer's disease and senile dementia in patients with Down's syndrome. *Am. J. Path.* **73**, 457–476 (1973).
8. Weisnewski, K.E., Weisnewski, M.H. & Wen, G.Y. Occurrence of neuropathological changes and dementia of Alzheimer's disease in Down's syndrome. *Ann. Neurol.* **17**, 278–282 (1985).
9. Korenberg, J. et al. Down syndrome phenotypes: The consequences of chromosomal imbalance. *Proc. natn. Acad. Sci. U.S.A.* **91**, 4997–5001 (1994).
10. McCormick, M.K. et al. Molecular approach to the characterization of the Down syndrome region of chromosome 21. *Genomics* **5**, 325–331 (1989).
11. Rahmani, Z. et al. Critical role of the D21S55 region on chromosome 21 in the pathogenesis of Down Syndrome. *Proc. natn. Acad. Sci. U.S.A.* **86**, 5958–5962 (1989).
12. Reeves, R.H. & Citron, M.P. Mouse Chromosome 16. *Mamm. Genome* **5**, S229–S237 (1994).
13. Epstein, C.J., Cox, D.R. & Epstein, L.B. Mouse trisomy 16: An animal model for human trisomy 21 (Down's syndrome). *Ann. N.Y. Acad. Sci.* **450**, 157–177 (1985).
14. Davison, M.T., Schmidt, C. & Akeson, E. Segmental trisomy of murine chromosome 16: A new model system for studying Down Syndrome. *Prog. clin. biol. Res.* **360**, 263–280 (1990).
15. Davison, M.T. et al. Segmental trisomy as a mouse model for Down Syndrome. *Prog. clin. biol. Res.* **384**, 117–133 (1993).
16. Dietrich, W.F. et al. A genetic map of the mouse with 4,006 simple sequence length polymorphisms. *Nature Genet.* **7**, 220–225 (1994).
17. Bendotti, C. et al. Neuroanatomical localization and quantification of cerebrovascular amyloid peptide RNA following *in situ* hybridization in the brains of normal, aneuploid, and experimentally lesioned mice. *Proc. natn. Acad. Sci. U.S.A.* **85**, 3628–3632 (1988).
18. Gearhart, J. et al. Mouse chimeras composed of trisomy 16 and normal (2N) cells: Preliminary studies. *Brain Res. Bull.* **16**, 815–824 (1986).
19. Sanberg, P., Moran, T. & Coyle, J. in *Experimental models of dementing disorders: A synaptic neurochemical perspective* (ed. Coyle, J.) 253–278 (Alan Liss, Inc., 1987).
20. Guilarte, T., Miceli, R. & Moran, T. Developmental effects of vitamin B-6 restriction on the locomotor behavior of rats. *Brain Res. Bull.* **34**, 31–40 (1991).
21. Bautista, J., Schwartz, G., delaTorre, D., Moran, T. & Carbone, K. Early and persistent abnormalities in rats with neonatally acquired Borna disease virus infection. *Brain Res. Bull.* **34**, 31–40 (1994).
22. Deliber, J.-M. et al. Report of the fourth international workshop on human chromosome 21. *Genomics* **18**, 735–744 (1993).
23. Cox, D.R., Burmeister, M., Price, E.R., Kim, S. & Myers, R.M. Radiation hybrid mapping: A somatic cell genetic method for constructing high resolution maps of mammalian chromosomes. *Science* **250**, 245–250 (1990).
24. Cheng, S.V. et al. Comparative mapping of DNA markers from the familial Alzheimer disease and Down syndrome regions of chromosome 21 to mouse chromosomes 16 and 17. *Proc. natn. Acad. Sci. U.S.A.* **85**, 6032–6036 (1988).
25. Miyabara, S., Gropp, A. & Winking, H. Trisomy 16 in the mouse fetus associated with generalized edema and cardiovascular and urinary tract anomalies. *J. exp. Zool.* **228**, 253–269 (1983).
26. Bucan, M. et al. Comparative mapping of 9 human chromosome 22q loci in the laboratory mouse. *Hum. molec. Genet.* **2**, 1245–1252 (1993).
27. Goldmuntz, E. et al. Microdeletions of chromosomal region 22q11 in patients with congenital conotruncal cardiac defects. *J. med. Genet.* **30**, 807–812 (1993).
28. Wisniewski, K.E., Dalton, A.J., Crapper-McLachlan, D.R., Wen, G.Y. & Wisniewski, H.M. Alzheimer's disease in Down syndrome: clinicopathologic studies. *Neurology* **35**, 957–961 (1985).
29. Goldgaber, D., Lerman, M.L., McBride, W.O., Saffiotti, U. & Gajdusek, D.C. Characterization and chromosomal location of a cDNA encoding brain amyloid of Alzheimer's disease. *Science* **235**, 877–880 (1987).
30. Tanzi, R.E. et al. Amyloid beta protein gene: cDNA, mRNA distribution and genetic linkage near the Alzheimer locus. *Science* **235**, 880–884 (1987).
31. Goate, A. et al. Segregation of a missense mutation in the amyloid precursor protein gene with familial Alzheimers disease. *Nature* **349**, 704–706 (1991).
32. Mulian, M. et al. A pathogenic mutation for probable Alzheimer's disease in the APP gene at the N-terminus of B-amyloid. *Nature Genet.* **1**, 345–347 (1992).
33. Lamb, B.T. et al. Introduction and expression of the 400 kilobase amyloid precursor protein gene in transgenic mice. *Nature Genet.* **5**, 22–30 (1993).
34. Games, D. et al. Alzheimer-type neuropathology in transgenic mice overexpressing V717F b-amyloid precursor protein. *Nature* **373**, 523–527 (1995).
35. Morris, R., Garrud, P., Rawlins, J. & O'Keefe, J. Place navigation impaired in rats with hippocampal lesions. *Nature* **297**, 681–683 (1982).
36. Wishart, J. in *The Psychobiology of Down Syndrome* (ed. Nadel, L.) 7–50 (M.I.T. Press, Cambridge, 1988).
37. Puschel, S. in *The Psychobiology of Down Syndrome* (ed. Nadel, L.) 199–216 (M.I.T. Press, Cambridge, 1988).
38. Marcel, M. & Armstrong, V. Auditory and visual sequential memory of Down Syndrome and nonretarded children. *Am. J. ment. Def.* **87**, 86–95 (1982).
39. Cabin, D.E., Hawkins, A., Griffin, C. & Reeves, R.H. YAC transgenic mice in the study of the genetic basis of Down syndrome. *Progr. clin. biol. Res.* **393**, 213–226 (1995).
40. Davison, M.T. & Akeson, E.C. An improved method for preparing G-banded chromosomes from mouse peripheral blood. *Cytogenet. Cell Genet.* **45**, 70–74 (1987).
41. Pittler, S. & Baehr, W. Identification of a nonsense mutation in the rod photoreceptor cGMP phosphodiesterase b-subunit of the *rd* mouse. *Proc. natn. Acad. Sci. U.S.A.* **88**, 8322–8326 (1991).
42. Kao, F.T. & Puck, K.T. Genetics of somatic mammalian cells, VII. induction and isolation of nutritional mutants in Chinese hamster cells. *Proc. natn. Acad. Sci. U.S.A.* **60**, 1275–1281 (1975).
43. Reeves, R.H. et al. Genetic linkage in the mouse of genes involved in Down syndrome and Alzheimers disease in man. *Molec. Brain Res.* **2**, 215–221 (1987).
44. O'Hara, B.F., Fisher, S., Oster-Granite, M.L., Gearhart, J.D. & Reeves, R.H. Developmental expression of the amyloid precursor protein, growth-associated protein 43, and somatostatin in normal and trisomy 16 mice. *Dev. Brain Res.* **49**, 300–304 (1989).
45. O'Hara, B.F. et al. Genetic mapping and analysis of somatostatin expression in snell dwarf mice. *Molec. Brain Res.* **4**, 283–292 (1988).
46. Camper, S.A., Saunders, T.L., Katz, R.W. & Reeves, R.H. The Pit-1 transcription factor gene is a candidate for the murine Snell dwarf mutation. *Genomics* **8**, 586–590 (1990).
47. Mjaatvedt, A., Citron, M.P. & Reeves, R.H. High resolution mapping of *D16Led1*, *Gart*, *Gas-4*, *Cbr*, *Pcp-4*, and *Erg* on mouse chromosome 16. *Genomics* **17**, 382–386 (1993).
48. Irving, N.G., Hardy, J.A. & Brown, S.D.M. The multipoint genetic mapping of mouse chromosome 16. *Genomics* **9**, 388–389 (1991).
49. Gregor, P. et al. Chromosomal localization of glutamate receptor genes: relationship to familial amyotrophic lateral sclerosis and other neurological disorders of mice and man. *Proc. natn. Acad. Sci. U.S.A.* **90**, 3053–3057 (1993).
50. Epstein, C.J. et al. Transgenic mice with increased Cu/Zn-superoxide dismutase activity: Animal model of dosage effects in Down Syndrome. *Proc. natn. Acad. Sci. U.S.A.* **84**, 8044–8048 (1987).
51. Watson, D.K. et al. Conserved chromosomal positions of dual domains of the ets protooncogene in cats, mice and humans. *Proc. natn. Acad. Sci. U.S.A.* **83**, 1792–1796 (1986).
52. Stashli, P. et al. Mx protein: Constitutive expression in 3T3 cells transformed with cloned Mx cDNA confers selective resistance to influenza virus. *Cell* **44**, 147–158 (1986).
53. Dietrich, W. et al. A genetic map of the mouse suitable for typing intraspecific crosses. *Genetics* **131**, 423–447. (1992).
54. Irving, N.G., Citron, M.P. & Reeves, R.H. The positions of twelve simple sequence repeat markers relative to reference markers on mouse chromosome 16. *Mamm. Genome* **4**, 364–367 (1993).
55. Sisodia, S.S., Koo, E.H., Hoffman, P.N., Perry, G. & Price, D.L. Identification and transport of full-length amyloid precursor proteins in rat peripheral nervous system. *J. Neurosci.* **13**, 3136–42 (1993).
56. Elstner, E.F. & Heupel, A. Inhibition of nitrite formation from hydroxylammonium chloride: A simple assay for Superoxide dismutase. *Analyt. Biochem.* **70**, 616–620 (1976).
57. Elroy-Stein, O., Bernstein, Y. & Groner, Y. Overproduction of human Cu/Zn-superoxide dismutase in transfected cells: extenuation of paraquat-mediated cytotoxicity and enhancement of lipid peroxidation. *EMBO J.* **5**, 615–622 (1986).